International Journal of Early Childhood Special Education (INT-JECSE)
DOI:10.48047/INTJECSE/V14I8.249 ISSN: 1308-5581 Vol 14, Issue 08 2022

FEM analysis using Quick-Field for a Silicon Rubber Composite Insulator

B. Mallikarjuna[1], G. Ezhilarasan[2], B. Basavaraja[3]

[1] Department of Electrical and Electronics Engineering, RNS Institute of Technology, Bengaluru, Karnataka, India.
[2]Department of Electrical Engineering, Jain Deemed to be University, Bengaluru, Karnataka, India.
[3] Professor, Department of Electrical Engineering, UBDTCE, Davanagere, Karnataka, India.

ABSTRACT: The electric and potential distribution characteristics of an outdoor porcelain insulator are examined in this research. Silicone rubber has been widely employed by power utilities since the 1980s as a replacement to porcelain and glass for high voltage insulators due to its superior contaminant performance. The solid air interface insulation is frequently involved in the breakdown of open-air high voltage insulators. As a result, understanding the field distribution surrounding high voltage insulators is critical for determining the electric field stress on the insulator surface, especially on the air side of the device. This study would investigate the electric field distribution of an activated silicone rubber high voltage insulator in this regard. Also shown are the simulation results of potential and electric field distributions along the surface of silicone rubber polymer insulators in both clean and contaminated circumstances. For this project, the finite element method (FEM) is used. Quick Field software is used to calculate the electric field distribution in two dimensions using the finite element approach. When water droplets are present on the insulator surface, the goal of this research is to identify the potential distribution and strength of the silicon rubber insulator
Keywords: FEM, Quick-Field, Potential distribution, silicon rubber insulator

1. INTRODUCTION

Silicon rubber composite insulators, that are now widely used, were not developed until the 1970s, and Germany was the first country to develop and use them. Composite insulators, such as silicon rubber insulator, provide greater advantages in application than traditional porcelain and glass insulators. This chapter will mostly examine issues relating to silicon rubber insulators for further information. Outdoor insulator expertise dates back to the establishment of telegraphic lines in the nineteenth century. Over hundreds of years of service and product development experience using high voltage insulators made of glass and porcelain materials has been accumulated [1-10].Until the development of porcelain ic replacements, porcelain and glass insulators totally dominated the market. In 1959, the United States of America produced the first polymeric insulator (epoxy), however it suffered from severe tracking and degradation[11-14].Similarly, for high voltage insulators, porcelain was the only material of option for an outdoor high voltage insulator for the first three quarters of the twentieth century. Shellac was a natural occurring resin and gum that was available in the early twentieth century. In 1907, Dr. Baekland invented synthetic phenol formaldehyde, which later became known as rubber. These two early porcelain materials had good interior qualities, but their track resistance was low since they were organic and contained a carbon backbone in their chain. Newer synthetic resins were produced later, in the 1930s and 1940s, and some of the first polymer insulators were built of butyl and acrylic materials [15-23].However, despite success in commercial aspect, they quickly become outdated due to increased costs, limited manufacture, limited adaptability, and, most significantly, insufficient performance for high voltage outdoor applications. The invention and use of cycloaliphatic epoxy helped to resolve the resin shortage, but it didn't solve the constant of thermal expansion problem at the fibreglass rod or housing interface [24-26].In warm, humid conditions, compounding materials to solve this compatibility delinquent resulted in depolymerization of the moulded sheds, resulting in electromechanical failure.

DOI:10.48047/INTJECSE/V14I8.249 ISSN: 1308-5581 Vol 14, Issue 08 2022

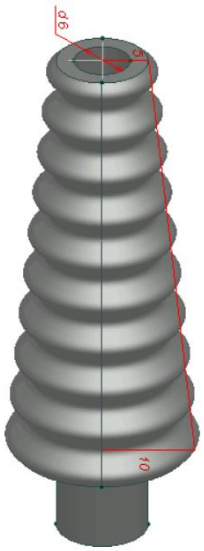

Figure 1 Structure of Porcelain insultor

Figure 1 depicts the structure of a porcelain insulator. A porcelain insulator's basic architecture is as follows: the load bearing structure is a fibre reinforced plastic (FRP) core attached to two metal fittings. To shield the FRP core from ecological stresses such as acid, acid, UV and ozone, well as to deliver a leakage distance, Weather conditions sheds are erected outside the FRP core when the insulator length is limited and the environment is polluted and moist. Silicone rubber is mostly utilised as a housing material for porcelain or composite insulators.

2. METHOD

A detailed simulation is required just before deploying a power system. Several simulation studies are available to establish power system parameters like electrical quantities such as voltage, current, and device power rating. Furthermore, investigations on the impact of flaws, such as security studies, are being carried out. Physical and environmental factors, on the other hand, are not mentioned in any of the studies presented here. As a result, there is an issue with power system dependability when transmission system insulators are placed in the out area. We employ Partial Differential Equation (PDE) simulation of the devices to explore the effects, which allows study electromagnetic effects as a function of temperature.

The electric field can be estimated by computing the potential distribution. The field can be determined by subtracting the electric potential distribution's negative gradient.

$$\mathrm{E} = -\nabla \mathrm{V} \quad (1)$$

Using maxwell's equation

$$\nabla \mathrm{E} = \nabla(-\nabla) = \frac{\rho}{\epsilon} \quad (2)$$

where, $\rho -$ resistivity Ω/m

$\epsilon -$ dielectric constant of the material $(\epsilon = \epsilon_0 \epsilon_\mathrm{r})$

$\epsilon_0 -$ dielectric space constant $\left(8.854 \times 10^{-12} \frac{\mathrm{F}}{\mathrm{m}}\right)$

$\epsilon_\mathrm{r} -$ relative dielectric material constant

Equation (1) is substituted in (2) Poisson's equation is as follows:

$$\epsilon . \nabla(\nabla V) = -\rho \quad (3)$$

Substitute $\rho = 0$ the equation (3) shows

$$\epsilon . \nabla(\nabla V) = 0 \quad (4)$$

The coordinates of the Cartesian system can be represented as an equation.$F(u)$

$$F(u) = \frac{1}{2}\int_D \left[\epsilon_x \left(\frac{du}{dx}\right)^2 + \epsilon_y \left(\frac{du}{dy}\right)^2\right] dxdy \quad (5)$$

where, ϵ_x and ϵ_y are x and y components of the dielectric constant. u is the electric potential.
By substituting in the case of isometric permittivity distribution $\epsilon = \epsilon_x = \epsilon_y$,
Equation (5) can be rewritten as follows: $F(u) = \frac{1}{2}\int_D \epsilon \left[\left(\frac{du}{dx}\right)^2 + \left(\frac{du}{dy}\right)^2\right] dxdy$ (6)

$$F^*(u) = \frac{1}{2}\int_D \omega\epsilon_0(\epsilon - j\epsilon.tg\delta) \left[\left(\frac{du^*}{dx}\right)^2 + \left(\frac{du^*}{dy}\right)^2\right] dxdy \quad (7)$$

$\omega -$ angular frequency,
$\epsilon_0 -$ perrmitivity of freespace
$tg\delta -$ tangent of dielectric loss angle
$u^* -$ complex potential
As seen below, a linear variation in electric potential is expected.

$$u_e(x,y) = \alpha_{e1} + x\alpha_{e2} + y\alpha_{e3} \quad (e = 1,2,3 \ldots n_e) \quad (8)$$

$u_e(x,y) -$ electric potential of arbitraty point
$D_e, \alpha_{e1}, \alpha_{e2}, \alpha_{e3}$ are the computational coefficient
by minimizing the following equation the the electric potential is calculated,

$$\frac{\partial F(u_i)}{\partial u_i} = 0; i = 1,2,..np$$

The total number of knots in the network is denoted by np.

3. RESULTS AND DISCUSSION

The silicon rubber based solid type bushing insulator of sinusoidal shape under nominal conditions are studied here. The voltage of the insulator is 10kV. The ground potential is kept as zero. The permittivity is given as 2.9 for silicon rubber and 1 for air. The sinusoidal shaped insulator is modelled in quick-field software. The Figure 1 shows the silicon rubber composite insulator designed in Quick-field software. The rectangular box is the air and the central structure is the insulator made of silicon rubber. The Figure 2 shows the Ground potential part of the insulator. The Figure 3 shows the High voltage part of the insulator. Then Figure 4 shows the Application of the PDE with triangular mesh. For the same figure Cross sectional view of figure 4 is shown. The Figure 6 shows the Field view of air. It can be seen that the side of ground potential is green and in the other end it is orange which shows the penitential is not reaching peak and the setup is still safe.

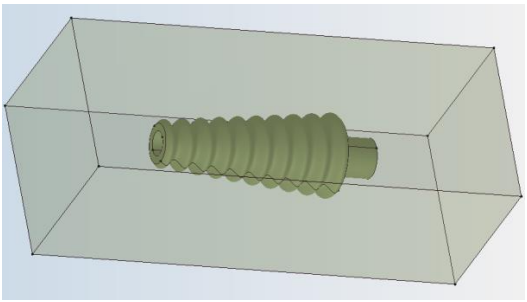

Figure 2 silicon rubber composite insulator designed in Quickfield software

DOI:10.48047/INTJECSE/V14I8.249 ISSN: 1308-5581 Vol 14, Issue 08 2022

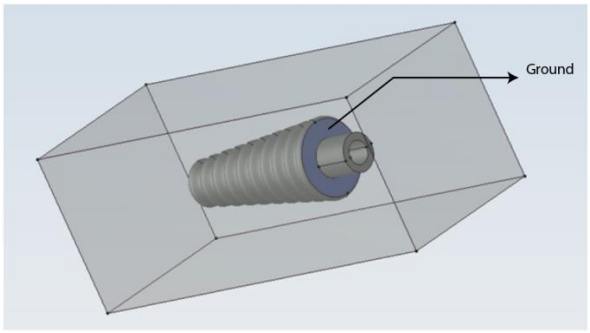

Figure 3 Ground of the insulator

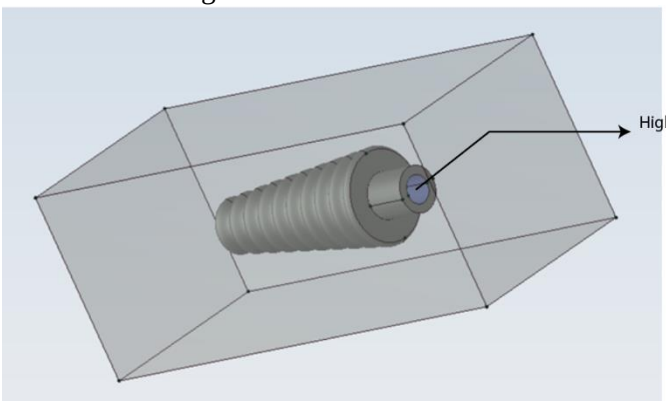

Figure 4 High voltage part of the insulator

The Figure 7 shows the voltage with respect to length of air. The peak value of the voltage is reached at the length of 0.2 m. The Figure 8 shows the Strength of the air. The strength drops at 0.2 and increases again. The Figure 9 shows the field view of the composite insulator model. The Figure 10 shows the bottom view of figure 9 this shows the ground is in blue colour. Then the Figure 11 shows the cross-sectional view of insulator. It shows that the insulator has the proper voltage distribution towards the ground. The Figure 12 shows the direction of the field.

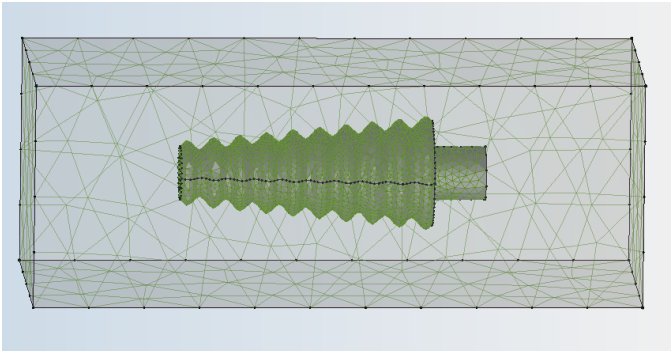

Figure 5 Applying the PDE with triangular mesh

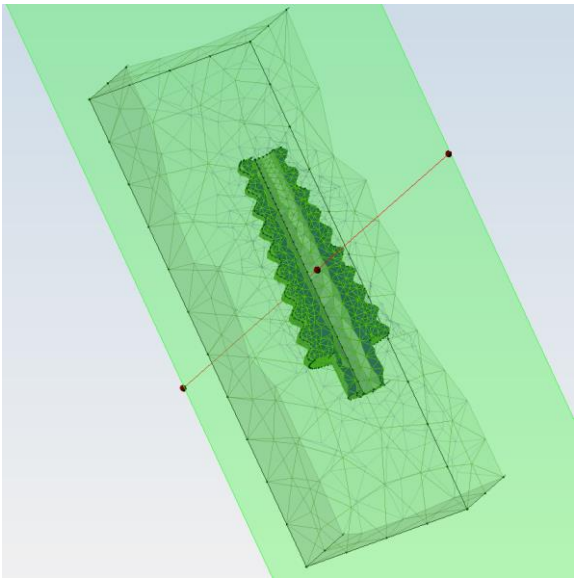

Figure 6 Cross sectional view of figure 4

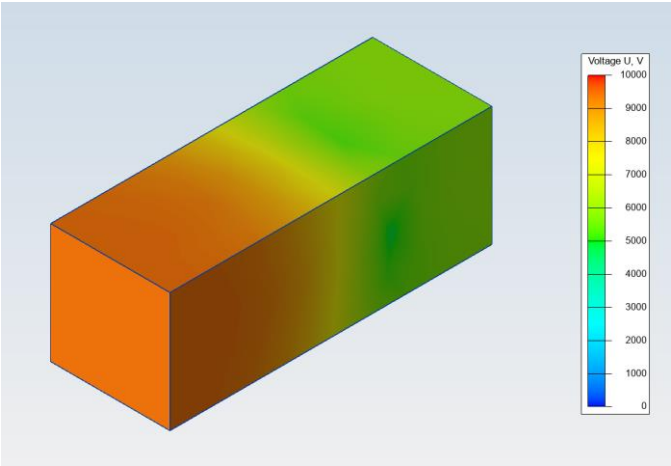

Figure 7 Field view of air

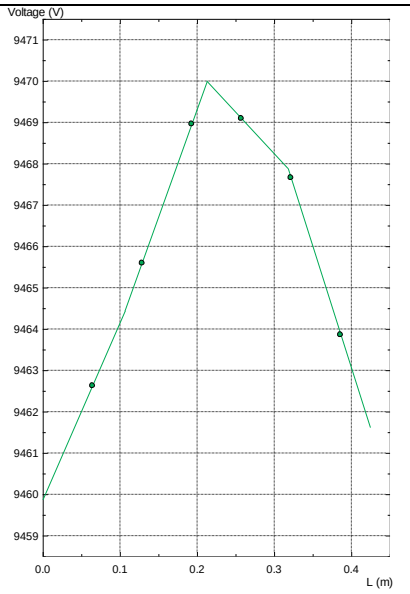

Figure 8 voltage with respect to length of air

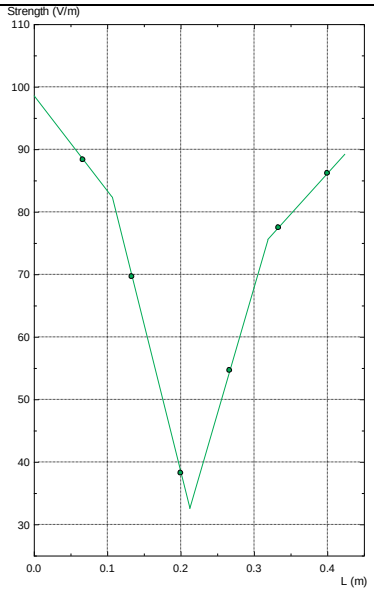

Figure 9 Strength of the air

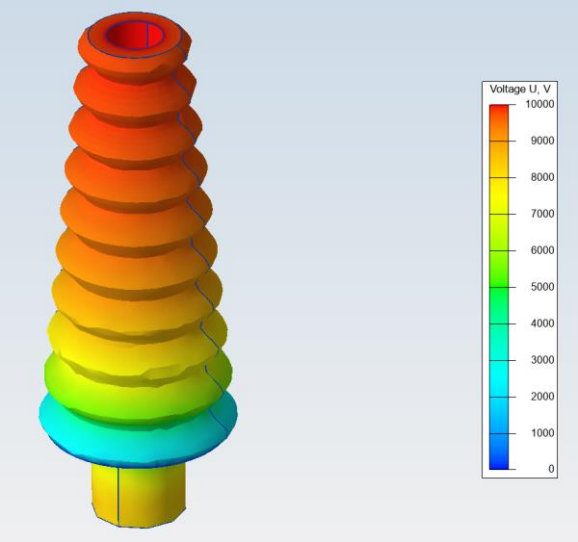

Figure 10 field view of the composite insulator model

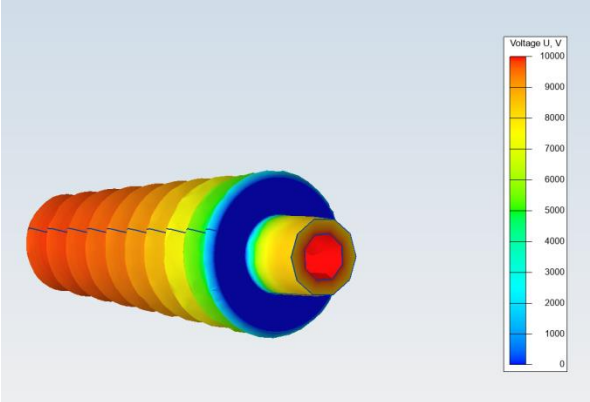

Figure 11 Bottom view of figure 10

The Figure 13 shows the Voltage with length of the insulator the voltage drops to zero at 0.6m and then stays on it still 0.9m. then the voltage starts to rise. The Figure 14 shows the strength of the insulator. The strength is more between 0.6m to 0.9m. The Figure 15 shows the 2D view of the insulator with air in field view. The Figure 16 depicts the zoomed view of figure 15. The red one is the high voltage area and blue is ground area. It shows that the composite material works well. The Figure 17 shows the strength of the insulator in field view. Mostly blue and around the ground area the strength is more.

DOI:10.48047/INTJECSE/V14I8.249 ISSN: 1308-5581 Vol 14, Issue 08 2022

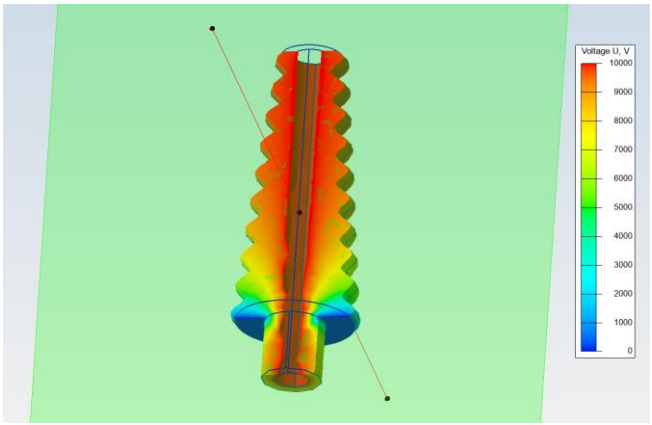

Figure 12 Cross Sectional view of insulator

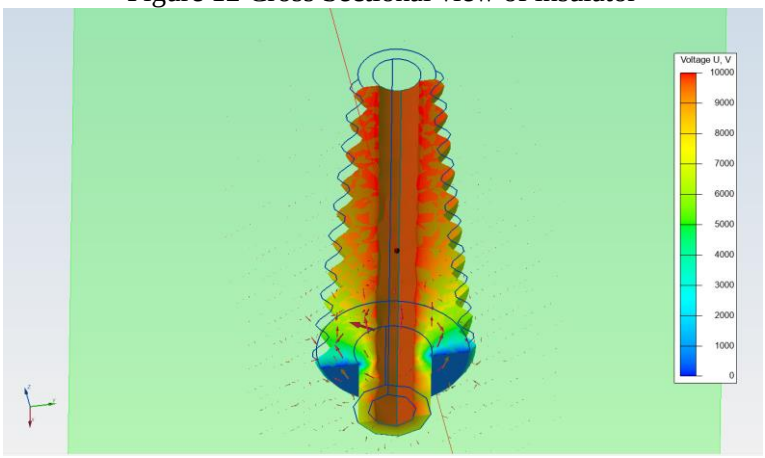

Figure 13 Direction of the field

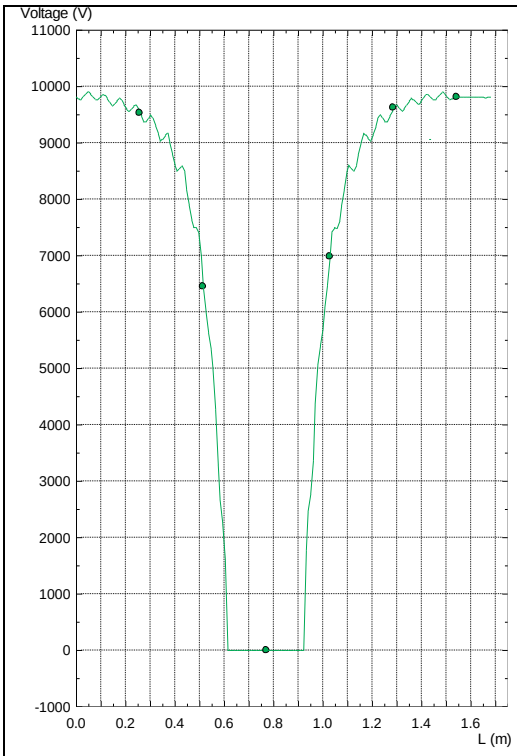

Figure 14 Voltage with length of the insulator

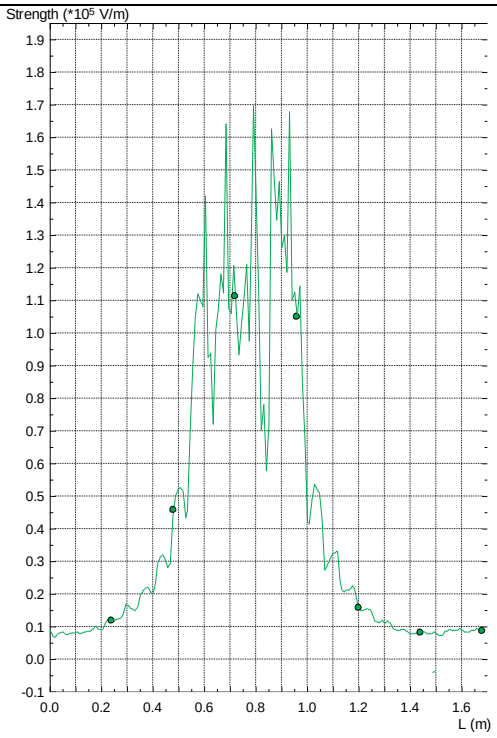

Figure 15 strength of the insultor

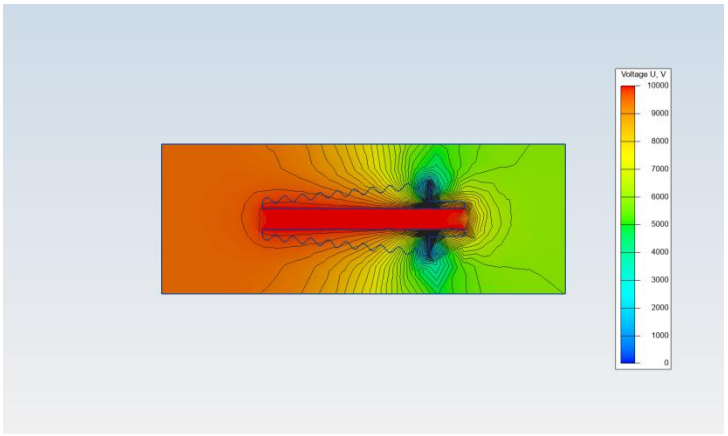

Figure 16 2D view of the insulator with air in field view

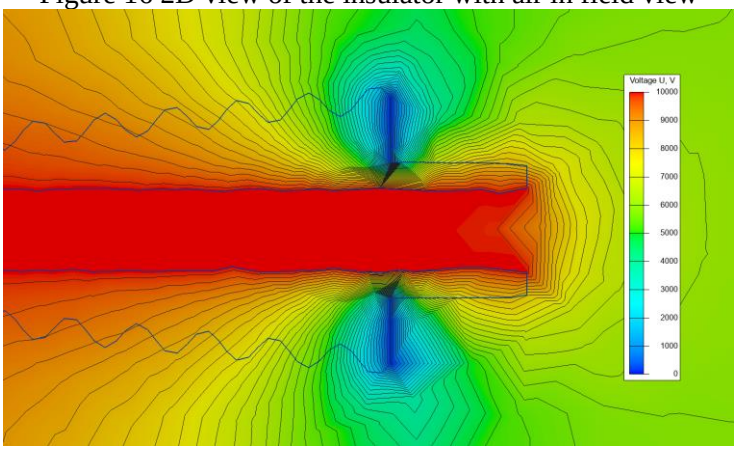

Figure 17 zoomed view of figure 15

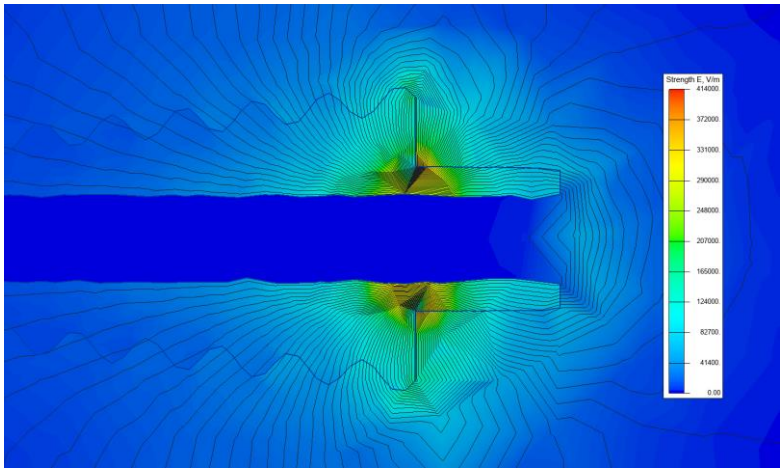

Figure 18 strength of the insulator in field view

4. CONCLUSION

The Quickfield simulation model is made of silicon rubber composite material and is used to test laboratory settings. The insulator is suspended in the air, with a sinusoidal insulator surface. The region of higher voltage is distinguished by its denser red colour. The zero potential zones are denoted by the blue colours. Before the real application, the 3D and 2D models are completed, and the property of the insulator may be determined from the graphs.

REFERENCES

[1] J. S. T. Looms. *Insulators for High Voltages*. London, United Kingdom: Peter Peregrinus Ltd, 1988, pp. 2-12.

[2] S. Chakravorti and H. Steinbigler, "*Boundary element studies on insulator shape and electric field around HV*
insulators with or without pollution," *IEEE Transactions on Dielectrics and Electrical Insulation*, vol.7, no.2, pp.169-176, Apr 2000.

[3] R. S. Gorur, E. A. Cherney, and J. T. Burnham, *Outdoor Insulators*, Ravi S. Gorur, Inc., Phoenix, Arizona, USA,
1999.

[4] CIGRE Taskforce 33.04.01: "*Polluted insulators: review of current knowledge*," CIGRE technical brochure 158, June 2000.

[5] A. S. Krzma, M. Albano, and A. Haddad, "*Comparative performance of 11kV silicone rubber insulators using artificial pollution tests*, "in 2015 50th International Universities Power Engineering Conference (UPEC),Stoke On Trent, United Kingdom, pp. 1–6, 2015.

[6] J. L. Rasolonjanahary, L. Krahenbuhl, and A. Nicolas, "*Computation of electric fields and potential on polluted insulators using a boundary element method*," *IEEE Transactions on Magnetics*, vol.28, no.2, pp.1473-1476, Mar 1992.

[7] A. S. Krzma, M. Albano, and A. Haddad, "*Flashover influence of fog rate on the characteristics of polluted silicone rubber insulators*," in 2017 52th International Universities Power Engineering Conference (UPEC), Crete, Greece, pp. 1–6, 2017.

[8] IEC 60507:2013, '*Artificial pollution tests on high-voltage ceramic and glass insulators to be used on a.c. systems'*, 3rd edition.

[9] M. Albano, A. S. Krzma, R. T. Waters, H. Griffiths, and A. Haddad, "*Artificial pollution layer characterization on conventional and textured silicone-rubber insulators*," in The 19th International Symposium on High Voltage Engineering (ISH), Pilsen, Czech Republic, 2015.

[10] M. Talaat: "Influence of Transverse Electric Fields on Electrical Tree Initiation in Solid Insulation", IEEE CEIDP 2010, pp. 313- 316, USA, October 17-20, 2010.

[11] M. Talaat: " A Simulation Model of Fluid Flow and Streamlines Induced by Non-Uniform Electric Field" IEEE, 14th MEPCON'10, pp. 371-375, Egypt, December 19-21, 2010.

[12] A. El-Zein, M. Talaat and M.M. El Bahy: "A Numerical Model of Electrical Tree Growth in Solid Insulation" IEEE TDEl, Vol. 16, No. 6; pp. 1724-1734, December 2009.

[13] A. El-Zein, M. Talaat and M.M. El Bahy: "A New Method to Predict the Electrical Tree Growth in Solid Insulation" Proceedings of the 16th ISH 2009, paper D-15, pp. 1-6, 2009.

[14] A. El-Zein and M. Talaat: "A New Model of Investigating the Electric Field in Dielectric Liquid for Streamer Initiation" J. Elec. Eng. (JEE) Vol. 10, No. 2, pp. 47-51, 2010.

[15] B. Marungsri, H. Shinokubo, R. Matsuoka and S. Kumagai: "Effect of Specimen Configuration on Deterioration of Silicon Rubber for Polymer Insulators in Salt Fog Ageing Test", IEEE TDEI Vol. 13, No. 1; pp.129-138, February 2006.

[16] B. Marungsri, W. Onchantuek, A. Oonsivilai and Kulworawanichpong, "Analysis of Electric Field and Potential Distributions along Surface of Silicon Rubber Insulators under Contamination Conditions Using Finite Element Method" World Academy of Science, Engineering and Technology 53, pp. 1353- 1363, 2009.

[17] William H. Hayt, Jr., Engineering Electromagnetics, 5th edition, McGraw-Hill Book Company, pp. 71-99, 1989.

[18] C. N. Kim, J. B. Jang, X. Y. Huang, P. K. Jiang and H. Kim: "Finite element analysis of electric field distribution in water treed XLPE cable insulation (1): The influence of geometrical configuration of water electrode for accelerated water treeing test", J. of Polymer Testing, Vol. 26, pp. 482 – 488, 2007.

[19] Kevin R.J. Ellwood, J. Braslaw: "A Finiteelement model for an electrostatic bell sprayer", Journal of Electrostatics, Vol. 45, pp. 1-23, 1998.

[20] Hergert A, Kindersberger J, Bar C, Barsch R (2017) Transfer of hydrophobicity of polymeric insulating materials for high voltage outdoor application. IEEE Trans DielectrElectrInsul 24(2):1057–1067. https://doi.org/10.1109/TDEI.2017.006146

[21] Ahmadi-Joneidi I, Shayegani-Akmal AA, Mohseni H (2017) Leakage current analysis of polymeric insulators under uniform and non-uniform pollution conditions. IET GenerTransmDistrib 11(11):2947–2957. https://doi.org/10.1049/iet-gtd.2016.2101

[22] Zhang Z, Wei D, Zhang D, Jiang X (2017) Effects of ring-shaped non-uniform pollution on outdoor insulation electrical property. IEEE Trans DielectrElectrInsul 24(6):3603–3611. https://doi.org/10.1109/TDEI.2017.006755

[23] Bychkov PN, Zabrodina IK, Shlapak VS (2016) Insulation contamination of overhead transmission lines by extreme service conditions. IEEE Trans DielectrElectrInsul 23(1):288–293. https://doi.org/10.1109/TDEI.2015.005323

[24] Zhang Z, Zhao J, Zhang D, Jiang X, Li Y, Wu B, Wu J (2018) Study on the dc flashover performance of standard suspension insulator with ring-shaped non-uniform pollution. IET High Volt 3(2):133–139

[25] Zhang Z, Zhang W (2016) AC flashover performance of various types of insulators under fan-shaped non-uniform pollution. IEEE Trans DielectrElectrInsul 23(3):1760–1768

[26] He Z, Gao F, Tu Z, Zhang Y, Chen H (2019) Analysis of natural contamination components and sources of insulators on±800 kV DC lines. Electr Power Syst Res 167:192–198. https://doi.org/10.1016/j.epsr.2018.10.033